Numerical Methods in Geomechanics (Innsbruck 1988), Swoboda (ed.)
© 1988 Balkema, Rotterdam. ISBN 90 6191 809 X

Finite element modelling of rapid drawdown

C.O.Li & D.V.Griffiths
Simon Engineering Laboratories, University of Manchester, UK

ABSTRACT: Aspects of finite element modelling of rapid-drawdown phenomena in soil slopes are discussed. The analyses involve finding the position of the steady-state phreatic surface through an earth dam, followed by sudden unloading due to reduction in water level on the upstream face. The analyses are performed in plane-strain using 8-noded quadrilateral elements, and it is shown that in the undrained analyses, oscillations in the computed pore pressures are considerably reduced by a form of selective reduced integration. It is found that the residual pore pressure distribution after the drawdown is not uniform with higher pore pressure concentration near the toe.

1. Introduction

A list of failures of earth dams between 1936-61 attributed to conditions set up during drawdown has been documented by Morgenstern (1963). Sudden drawdown leads not only to possible stability problems on the upstream slopes of earth dams, but may also induce slides in the natural slopes of the reservoir area. In addition, Koppejan et al(1948) suspected that the drawdown mechanism during tidal recession was one of the causes of coastal flow slides. Jones et al (1961) also recorded that landslides on the banks of the Franklin D. Roosevelt lake were more numerous after a lowering of the level of water impounded behind the Grand Coulee Dam.

The mechanism of drawdown may be considered in stages. First the pore pressure distribution in an earth dam prior to lowering of the reservoir level is governed by the steady seepage condition where the soil has consolidated under its own self weight. Following this, the lowering of the water level causes changes in the pore pressure as a result of the unloading during drawdown establishing new boundary conditions for seepage through the dam. During this transient phase, the free-surface gradually adjusts to a new equilibrium position by dissipating the excess pore pressures. As a result, the effective stresses increase with time as does the factor of safety of the upstream slope.

In fill materials of 'low' permeability, a significant amount of time is required for equilibriumn to be reached after drawdown. The most critical time however, occurs immediately after drawdown hence an 'undrained' assumption is conservative. The 'rapid drawdown' mechanism can therefore be reviewed as a consolidated (steady seepage) - undrained (rapid drawdown).

2. Analyses of Drawdown

Early attempts to analyse embankment stability during drawdown were carried out by Mayer (1936). An assumed failure plane in conjunction with the Method of slices led to a resultant shear force which implied failure if it was greater than the shear resistance of the soil. Lowe (1960) proposed a slip circle again in conjunction with the Method of slices. This more refined approach obtained an undrained shear strength (C_u) accounting for the anisotropically consolidated soil such as that occuring in elements of soil under high reservoir level prior to drawdown. Morgenstern (1963) recognised that the change in loading due to drawdown will induce immediate changes in pore pressure prior to consolidation. This concept is consistent with Skempton (1954) who first established the well-known equations in which changes in pore pressure under undrained conditions are related to changes in total stresses via the pore pressure parameters A and B. Using this approach, Morgenstern used slip circle methods to produce a set of stability charts for upstream slopes with various inclination and shear strength parameters (c', ϕ') (Morgenstern 1963).

Very few finite element analyses of the rapid drawdown problem have been reported. Desai (1977) and Li (1983) proposed a finite element procedure for seepage and stability of earth dams during transient flow where pore pressures begin to dissipate following drawdown. In these analyses, the effects of the fluid and solid phases were not coupled, but superimposed during the analyses. In the present work, the authors present a more rigorous approach in which coupling between the phases is considered. The analysis can be considered in two parts; a steady state solution followed by undrained unloading.

3. Method of Analysis

3.1 Steady Seepage

Initially, a finite element procedure is derived to locate the position of the free surface prior to drawdown. There are two basic methods for doing this; the mesh adaptive methods e.g. Taylor and Brown (1967), Finn (1967), Witherspoon and Neuman (1970), Smith and Griffiths (1987) and the fixed mesh methods e.g. Desai (1976), Bathe (1979). The fixed mesh approach has been used in the present study for the following reasons:

(i) The same mesh can be used for both the seepage and stress analyses.

(ii) The mesh adaptive methods can run into difficulties in the case of layered soils with horizontal interfaces and for soils involving non-homogeneous permeabilities. It is also difficult to assign appropriate material properties when the free surface crosses on interface. (Li 1983).

(iii) The mesh may become so distorted that the error due to the finite element approximation becomes significant.

3.2 Slope Stability

Gravity loads are applied to the slope and constant stiffness iterations (modified Newton-Raphson) are used to obtain a converged solution. The viscoplastic iterative technique is described elsewhere (e.g Zienkiewicz 1977, Grifiths 1980).

In the present analyses, after location of the steady state seepage line, the steady residual pore pressure is applied as nodal water force vector together with the gravity loading due to soil self weight and the upstream force corresponding to the water level prior to drawdown. This generates the consolidated stresses corresponding to the steady state condition. These stresses then act as the intial stress state prior to rapid (undrained) drawdown unloading.

4. The Fixed Mesh Method

Consider 2-D steady seepage through a dam as shown in Figure 1.

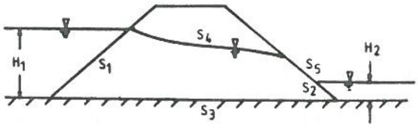

Figure 1: Boundary Conditions

For no sources or sinks within the system, the governing equation is due to Laplace of the form:

$$\frac{\partial}{\partial x}\left(k_x \frac{\partial \phi}{\partial x}\right) + \frac{\partial}{\partial y}\left(k_y \frac{\partial \phi}{\partial y}\right) = 0 \qquad (1)$$

where ϕ = potential, k_x, k_y = permeabilities in x and y directions. The boundary conditions from Figure 1 can be summarised as follows:

$$\begin{array}{ll} S1 & \phi = H_1 \\ S2 & \phi = H_2 \\ S3 & \frac{\partial \phi}{\partial n} = 0 \\ S4 & \phi = y, \ \frac{\partial \phi}{\partial n} = 0 \\ S5 & \phi = y \end{array} \qquad (2)$$

Boundary conditions S1, S2, S3 can be easily satisfied in the finite element formulation (e.g. Smith and Griffiths 1987). On the free surface, the location of S4 is unknown 'a priori' and condition S5 depends on S4. The method used is to set the permeability to zero, or in practice a very small number, when the computed pressure becomes negative (i.e. above the free surface) during each iteration (Bathe 1979, Werner 1986). A smoothing technique proposed by Werner (1986) is also used to avoid undesirable oscillation which occurs when a sudden change in permeability is encountered (Figure 2).

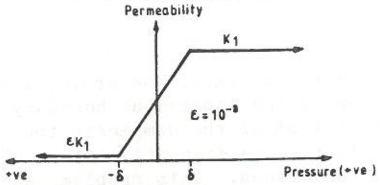

Figure 2: Permeability–Pressure Relationship

The length of the seepage surface S5 is estimated on each iteration by minimising the net outflow given by the expression

$$\frac{\partial}{\partial x}\left(k_x \frac{\partial \phi}{\partial x}\right) + \frac{\partial}{\partial x}\left(k_y \frac{\partial \phi}{\partial y}\right) \qquad (3)$$

5. Simplified Biot formulation for 2-D undrained Analysis

Assuming for the moment an elastic soil skeleton and an incompressible pore fluid we get the following equilibrium equation:

$$\frac{\partial \sigma'x}{\partial x} + \frac{\partial \tau xy}{\partial y} + \frac{\partial u}{\partial x} = F_x \qquad (4)$$

$$\frac{\partial \sigma'y}{\partial y} + \frac{\partial \tau xy}{\partial x} + \frac{\partial u}{\partial y} = F_y \qquad (5)$$

where u = excess pore pressure, F_x, F_y = body forces.

With reference to the pore fluid, Darcy's law and continuity conditions can be summarised thus:

$$\frac{\partial}{\partial x}\left(k_x \frac{\partial \phi}{\partial x}\right) + \frac{\partial}{\partial y}\left(k_y \frac{\partial \phi}{\partial y}\right) = \frac{\partial}{\partial t}\left(\varepsilon_x + \varepsilon_y\right)$$

(Where plane strain conditions are implied). For saturated undrained conditions, no volume change takes place hence only the stress equilibrium equation is required which can be written as:

$$\underline{B}^T\underline{\sigma}' + \underline{B}^T\underline{U} = \underline{F} \qquad (6)$$

where $\underline{B}^T = \begin{vmatrix} \frac{\partial}{\partial x} & 0 & \frac{\partial}{\partial y} \\ 0 & \frac{\partial}{\partial y} & \frac{\partial}{\partial x} \end{vmatrix}$ $\qquad \underline{u} = \begin{vmatrix} u \\ u \\ 0 \end{vmatrix}$

$\underline{\sigma}' = \begin{vmatrix} \sigma'x \\ \sigma'y \\ \tau xy \end{vmatrix}$

Relating stress to strains we get:

$$\underline{\sigma}' = \underline{D}'\underline{\varepsilon}, \quad \underline{u} = \underline{D}^u \underline{\varepsilon}^u \qquad (7)$$

where $\underline{D}^u$ = stress strain matrix of the pore fluid

$\underline{D}'$ = effective stress strain matrix of the soil skeleton

For undrained conditions, there is no relative movement between the pore water and soil skeleton, hence:

$$\underline{\varepsilon} = \underline{\varepsilon}^u \qquad (8)$$

In addition, we assume that the pore pressures contribute only to direct stresses (and not at all to shear stresses) hence:

$$\underline{D}^u = K_A \begin{vmatrix} 1 & 1 & 0 \\ 1 & 1 & 0 \\ 0 & 0 & 0 \end{vmatrix} \qquad (9)$$

where K_A is the apparent Bulk Modulus of the pore fluid, usually assigned a large, but finite value (Griffiths 1985). The analysis now amounts to a 'penalty' formulation in which the total Poisson's ratio of the soil/fluid system approaches 0.5.

We can now write a simplified version of the Biot formulation for an undrained analysis. From equations (6) and (7).

$$\underline{B}^T(\underline{D}' + \underline{D}^u)\,\underline{\varepsilon} = \underline{F} \qquad (10)$$

or

$$\underline{B}^T\,\underline{D}\,\underline{\varepsilon} = \underline{F} \qquad (11)$$

where $\underline{D} = \underline{D}' + \underline{D}^u$

represents the total stress/strain matrix.

A similar formulation was first obtained by Naylor (1974). Although this method can be used to estimate pore pressures from equation (7), it has been found that the values obtained at the Gauss points tend to oscillate. A technique for smoothing these oscillations is now described.

6. An Integration Technique for the Pore Pressure Smoothing

For nearly incompressible material such as saturated soils during undrained loading, 'reduced' integration is commonly used in conjunction with 8-node elements to avoid the troublesome volumetric portion of the strain energy and to overcome 'mesh locking' (e.g. Fried 1974, Zienkiewicz 1977). Reduced integration relaxes the number of constraints imposed by satisfying the incompressibility condition only at the Gauss points. As a result, the overall performance of the element may be improved, but errors are introduced into the volumetric strain energy by relaxing the 'zero' volume change condition throughout the element. Although these errors may be small in magnitude, they may become significant as pore pressures after multiplication by a 'large' fluid bulk modulus.

In the present work, it is proposed that exact integration is used to obtain the total strain energy, but stresses will still be sampled at the 'reduced' integration point locations. The reduced integration points for stresses will continue to be used because:

(i) Computation time is reduced when using constant stiffness iterations in which the global stiffness matrix is formed once only.

(ii) The reduced integration points are the best positions for assembling stresses for either reduced or exact integrations schemes as observed by Zienkiewicz (1977).

The integration technique described above will be confirmed by numerical examples in the next section. It can be shown that the particular application described in this paper does not suffer from 'mesh locking' when using exact integration.

Discussions

Examples of the proposed fixed mesh method using 8-node quadrilateral elements with 'reduced' (2 x 2) integration are presented in Fig. 3 and 4. The free surface solutions are observed to converge rapidly in all the cases and agree very well with other published solutions. With the given unit permeabilities in x- and y- directions, the calculated flow rate for the vertical homogeneous dam in fig 3 is 4.59 compares favourably with the result 4.55 from Ligget (1977). For the

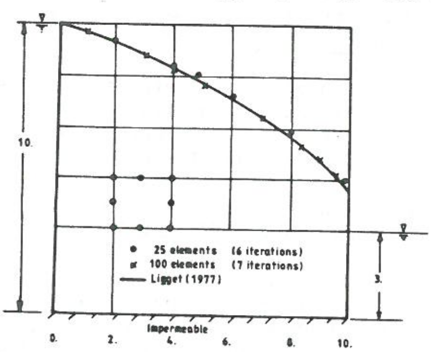

Figure 3: Compare Free Surface with published solution

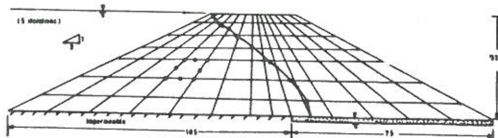

Figure 4: *FEM* Free Surface solution for a sloped embankment

example with horizontal toe drain, the point at which the impervious boundary along the bottom of the dam meets the drain will create a discontinuity in the boundary conditions. This problem can be avoided by representing the boundary meeting point with two nodes, one connected to the element above the impervious boundary with the other, with zero prescribed pressure, connected to the element above the drain.

In stress analysis for slope stability during rapid drawdown, the element is assumed to be elastic-perfectly plastic with the Mohr-Coulomb failure criterion. Non-linearity introduced by the plasticity is accounted for using the viscoplastic method. Non-dilatant soil behaviour is assumed and non-associated flow rule is used. The factor of safety (FOS) is defined as $C_f' = C'/FOS$, $\phi_f' = \text{Arc tan} (\tan \phi' /FOS)$. An example of a fully submerged slope under complete drawdown is used to study the effect of the magnitude of KA (Fig. 5). It shows that the FOS remains unchanged throughout the range of KA = 25 E' to 1000E'. However, the pore pressure response due to the drawdown unloading suffers severe oscillations. The magnitude of these oscillations increases with increasing KA (Fig. 6). This is thought to be due to the errors involved in the volumetric strain ($\Delta\varepsilon_v$).

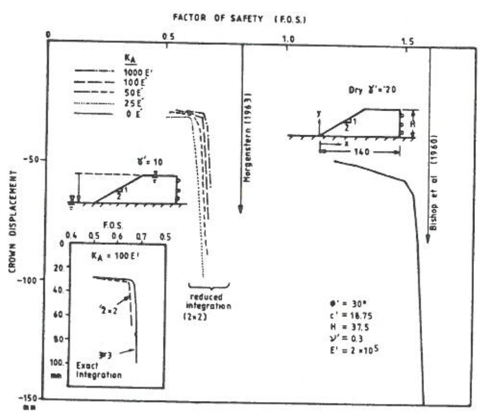

Figure 5: Effect of K_A on *F.O.S.* : Compare with published results

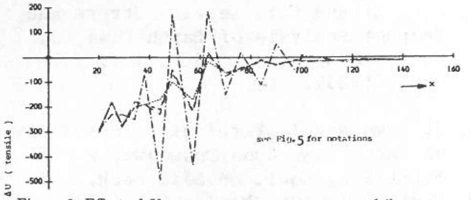

Figure 6: Effect of K_A on pore pressure response at failure at $y = 8.9$.

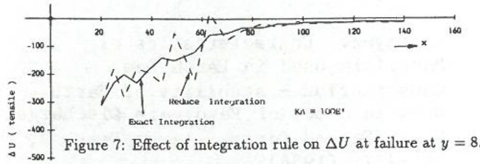

Figure 7: Effect of integration rule on ΔU at failure at $y = 8.9$.

Since the pore-pressure is $\Delta U = KA.\ \Delta\varepsilon_v$, increasing KA will magnify the error in the pore pressure and hence the oscillations. The error in the volumetric strains is a consequence of 'relaxing' the element using 'reduced' integration, and can be reduced if exact integration is used. This is confirmed in Fig. 7. Comparing the FOS of the fully submerged slope under complete rapid drawdown with published results, the coupled FEM solution (FOS = .67) underestimates that from Morgenstern (FOS = .82) by about 18% (Fig. 5). The 'dry' solution however, agrees exactly with that by Bishop and Morgenstern (1960). A close examination of the residual pore pressure distribution after complete drawdown of the coupled solution shows a non-uniform distribution with higher value concentrated near the toe areas (Fig. 8). The pore pressures obtained in the present work correspond to an elastic, perfectly plastic (non-dilative) soil model. Morgenstern (1963) assumed a uniform residual pore pressure distribution given by $\gamma_w.h$ (Fig. 8) and this simplified approach leads to an overestimation of the factor of safety. In very loose materials during undrained shear, the pore pressures would be greater still, leading to even lower factors of safety. Fig. 9 shows the results of the coupled analysis for upstream failure due to different amounts of drawdown. Both a single slope and a double sided embankment have been considered and the results agree well with Morgenstern (1963).

Conclusions

The paper has discussed coupled FEM and fixed mesh methods for rapid drawdown analysis. It has been shown that the residual pore pressure distribution after the drawdown is not uniform with pore pressure tending to the highest near the toe. This led to the Factors of Safety lower than those obtained using traditional methods. The oscillations in the pore pressure response due to using 'reduced integration' can be greatly improved by using exact integration to form the global stiffness matrix.

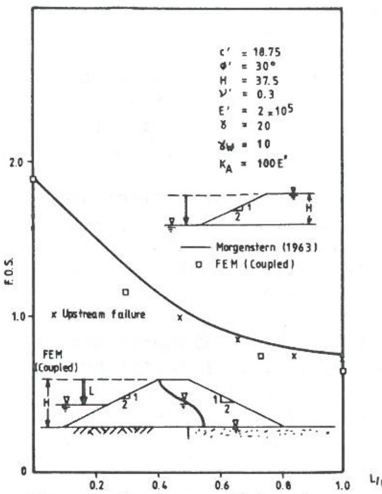

Figure 9: Compare rapid drawdown solutions with published results.

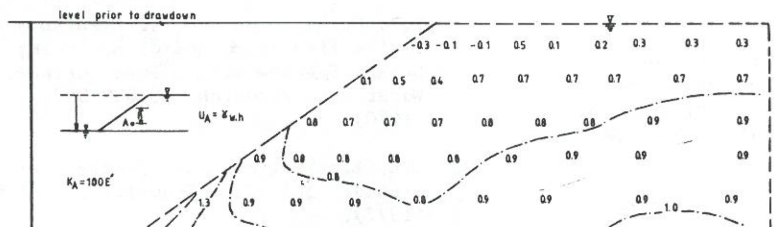

Figure 8: $\frac{U_{FEM}}{\gamma_w.h}$ distribution after complete rapid drawdown using exact integration rule.

References

(1) A.W. Bishop, and N. Morgnestern, :Stability coefficients for earth slopes, Geotech. 10, 129-150 (1960).

(2) K.J. Bathe and M.R. Khoshgoftaar, :Finite Element Free Surface Seepage Analysis without mesh iteration, Int. J. Num. Anal. Meth. Geom., 3, 13-22 (1979).

(3) C.S. Desai: Finite Element Residual Schemes for Unconfined flow, Int. J. Num. Meth. Engng, 10, 1415-1418 (1976).

(4) C.S. Desai: Drawdown Analysis of slopes by Numerical Method", J. Geot. Engng, Div., ASCE, 103, 667-676 (1977).

(5) W.D.L. Finn: Finite-Element analysis of seepage through Dams, J. Soil Mech. Found. Div., ASCE, 93, 41-48 1967.

(6) D.V. Griffiths: Finite Element analysis of walls, footings and slopes, Ph.D, thesis, University of Manchester, Simon Eng. labs. (1980).

(7) D.V. Griffiths: The effect of pore-fluid compressibility on failure loads in the Elasto-plastic soil" Int. J. Num. and Anal. Meth. Geom. 9, 253-259 (1985).

(8) I. Fried: Finite Elements Analysis of Incompressible Material by Residual Energy Balancing, Int. J.Solids and Structures, 10, 993-1002, (1974).

(9) F.O. Jones, D.R. Embody, and W.L. Peterson: Landslides along the Columbia River Valley, Northeaston, Washington, Professional Paper No 367, U.S. Geological Survey, Washington (1961).

(10) A.W. Koppejan, B.M. van Wamellen, and L.J.H. Weinberg: Coastal flow slides in the Dutch province of Zeeland, Proc. Second Int. Conf. Soil Mech., 5, 89-92, (1948).

(11) J.A. Ligget: Location of free surface in porous media, J. Hydr. Div. proc. ASCE, HY4, 353-365, (1977).

(12) G.C. Li and C.S. Desai: Stress and Seepage Analysis of Earth Dams, J. Geot. Engng. Div., ASCE, 109, 947-960, (1983).

(13) J. Lowe and L. Karafiath: Stability of Earth Dams upon Drawdown, Proc. First Pan. Conf. on Soil Mech. and Finite Element, Mexico City, 537-552, (1960).

(14) A. Mayer: Characteristics of Materials used in Earth Dam Construction - stability of Earth Dams in cases of Reservoir Discharge, Proc. Second Congr. Large Dams, 4, 295-327, (1936).

(15) N. Morgenstern: Stability Charts for Earth Slopes during Rapid Drawdown. Geotech. 13, 121-131, (1963).

(16) D.J. Naylor: Stresses in nearly incompressible materials by Finite Elements with application to the calculation of excess pore pressure. Int. J. Num. Meth. Engng. 8, 443-460 (1974).

(17) I.M. Smith and D.V. Griffiths: Programming the Finite Element Method, 2nd Edition, Wiley and Sons, to be published in 1987.

(18) A.W. Skempton: The pore-pressure coefficient A and B, Geotech. 4, 143-147, (1954).

(19) R.L. Taylor and C.B. Brown: Darcy flow solutions with a Free Surface. J. Hydr. Div. Proc. ASCE, 93, 25-33, (1967).

(20) H. Werner and E. Rank: An Adaptive Finite Element approach for the Free Surface Seepage problem. Int. J. Num. Meth. Engng, 23, 1217-1228 (1986).

(21) P.A. Witherspoon and S.P. Neuman: Finite Element Method of Analysing Steady Seepage with a Free Surface. Water Res. Research, 6, 889-897, (1970).

(22) O.C. Zienkiewicz, The Finite element method. 3rd ed. McGraw-Hill, London, (1977).